18TH WORLD CONFERENCE ON EARTHQUAKE ENGINEERING
WCEE2024
MILAN

MILAN, ITALY
30TH JUNE - 5TH JULY 2024
www.wcee2024.it

ACCOUNTING FOR GROUND MOTION DIRECTIONALITY IN REGIONAL SEISMIC RISK ASSESSMENT

A. Poulos[1] & E. Miranda[2]

Stanford University, Stanford, USA, apoulos@stanford.edu

[2] Stanford University, Stanford, USA

Abstract: *Regional seismic risk assessment estimates the losses or performance in general of a group of spatially distributed structures when subjected to earthquake events. A critical step of this assessment is to estimate the response or damage of a large number of structures given distinct ground motions at each site, which is usually characterized using a measure of ground motion intensity at each site, such as spectral accelerations. However, these intensity measures actually vary significantly with changes in orientation within the horizontal plane, a phenomenon known as ground motion directionality. This variation is almost always neglected both in seismic hazard analysis and in regional seismic risk assessment, where horizontal ground motion intensity at a given site is simplified by using a measure of central tendency from all horizontal orientations. However, the directionality of ground motions affects structural response because, due to the arrangement of lateral load-resisting elements, most buildings have two orthogonal principal horizontal orientations, which makes their structural properties orientation-dependent. This work studies the effect of accounting for ground motion directionality in regional risk assessment using a set of high-rise buildings as a testbed. A variance-based sensitivity analysis is performed to compare the contribution to the output variance of ground motion directionality with that of other sources of uncertainty, such as uncertainties related to structural response modeling and damage assessment. Ground motion directionality is found to be a very important source of uncertainty and its contribution increases as more buildings are considered in the analysis. Finally, the impact of urban street orientations is also studied, showing that perfectly orthogonal grid layouts, where all buildings have the same principal orientations, magnify directionality effects and increase the variance of output risk variables.*

1. Introduction

Ground motion intensity, usually characterized in earthquake engineering by a response spectral ordinate, can vary significantly with horizontal orientation, a phenomenon known as ground motion directionality. For example, spectral accelerations at 1 and 10 s are, on average, 55% and 102% higher in the orientation of maximum spectral response than in the perpendicular orientation, respectively (Poulos et al., 2022). This variation is almost always neglected by current regional seismic risk analysis procedures, probably because: (1) the ground motion models used to estimate ground motion intensity use a single scalar value for horizontal intensity, such as the median from all orientations (i.e., RotD50; Boore, 2010); (2) most models used to estimate structural response of buildings also use scalar intensity measures; and (3) until recently, there was a lack of models that can be used to estimate spectral ordinates at specific horizontal orientations, such as those recently proposed by the authors (e.g., Poulos and Miranda, 2022; Poulos and Miranda 2023b).

Most buildings have two principal horizontal orientations that are perpendicular to each other because of the arrangement of their lateral load-resisting elements and their geometry. Additionally, many damageable building components such as beams, bracing elements, structural walls, façades, and interior partition walls are aligned to the principal orientations of each building, such that estimating the peak demands in these directions is a primary concern. Moreover, groups of buildings within a city usually have similar principal orientations because they tend to follow the orientations of streets, which are arranged in perpendicular grid layouts for many cities in different parts of the world (Boeing 2019). Since the orientations of maximum horizontal spectral response tend to be similar at locations close to each other, especially at long periods (Filippitzis et al., 2021; Poulos and Miranda, 2023a), spectral accelerations in the principal orientations of the buildings are correlated due to these directionality effects. Moreover, the seismic responses of the buildings, and therefore their possible damages and losses, are controlled by the ground motion intensities in these two orientations, and hence they are also correlated due to directionality. This correlation in turn increases the variability of seismic losses when aggregating a group of buildings. This effect is not captured by current regional seismic risk analysis methods because they do not model ground motion directionality nor consider the orientations of buildings. In other words, if the orientations of the buildings were altered the method would produce the same results.

This study quantifies the effect of considering ground motion directionality and the orientations of buildings when estimating the seismic loss of a group of buildings within a city. The probabilistic method used to estimate seismic losses is simulation-based and considers several sources of uncertainty, such as those related to ground motion directionality and several others that are usually considered by previous regional seismic risk analysis methods. A variance-based sensitivity analysis is used to compare how the different sources of uncertainty, and especially those related to directionality, contribute to the output variance of the method. A set of 196 high-rise buildings subjected to an example earthquake is used as a testbed of the method in order to perform the comparisons.

2. Methods

The repair cost of a group of spatially distributed buildings within a city was estimated using a Monte Carlo method based on stochastic simulations. The method is summarized in the diagram of Figure 1, which presents the input data required for the analysis and the intermediate and final outputs that are generated. The starting point is to define an earthquake scenario, which, together with the location of the buildings and the soil properties of the sites, is used to sample RotD50 response spectra for 5% damping at each site of interest. These RotD50 spectra are then used to sample 5%-damped response spectra in the two principal orientations of each building. The modal properties of each building (i.e., periods and damping ratios) are then sampled separately and used to obtain spectral accelerations for each mode. Structural responses (i.e., peak floor acceleration and interstory drift ratios) of each building are then estimated using a continuous beam model. These responses are then used to estimate the damage of different structural and non-structural elements within the buildings using a story-based approach. The damages are then converted to repair costs and expressed as a proportion of the replacement cost of the complete story. Finally, the normalized repair costs of all stories and buildings are added up to obtain the total number of lost stories for the whole group of buildings.

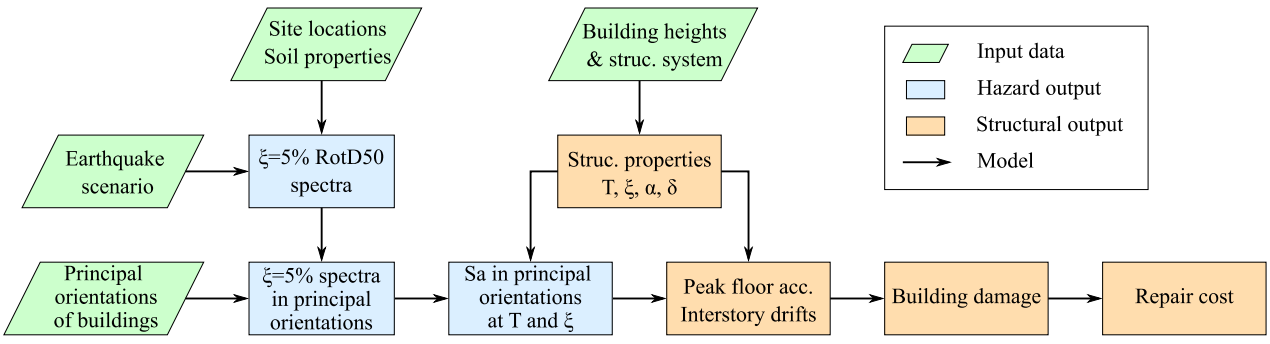

Figure 1. Summary of the method used to compute regional seismic losses.

This study applies the method shown in Figure 1 to a testbed consisting of a set of 196 buildings arranged in a 14 by 14 grid with a spacing of 200 m, as shown in Figure 2. For the sake of simplicity, all buildings are 100 m tall, have a structural system consisting of steel-braced frames, and have 30 stories each. The site properties were assumed to be the same for all buildings, with an average share wave velocity in the top 30 m of soil of 400 m/s. The seismic losses were computed for a M_w 7.0 strike-slip earthquake with an epicenter occurring 21 km from the center of the building grid.

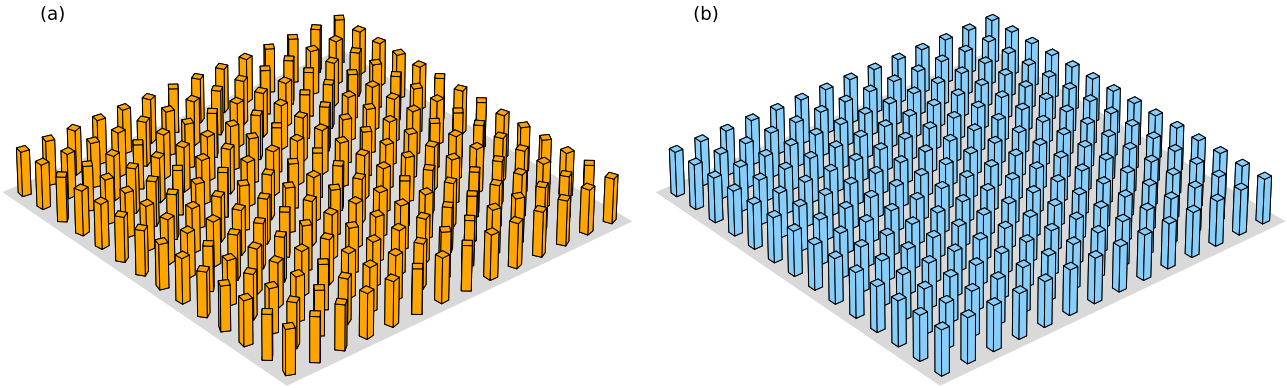

Figure 2. Example of building orientations used in the testbed: (a) sampled from a uniform probability distribution and (b) oriented in a north-south/east-west grid.

2.1. Ground motion modeling

The method starts by sampling 5%-damped response spectra at the location of each building using the ground motion model (GMM) developed by Boore et al. (2014). This sampling depends on the selected earthquake scenario, the location of the buildings, and the site properties. The sampled spectra consider spatial and spectral correlations between response spectral ordinated by using the models developed by Heresi and Miranda (2019) and Baker and Jayaram (2008), respectively.

The GMM provides statistical properties of median spectral accelerations from all horizontal orientations, that is, the RotD50 intensity. Thus, the sampled spectra correspond to RotD50 estimates. The model developed by Poulos and Miranda (2022) is then used to transform the RotD50 spectra into spectra in both principal horizontal orientations of each building, which is depicted schematically in Figure 3. The first step consists of selecting an orientation of RotD100, that is, of the maximum spectral acceleration in the horizontal plane. In this study, the orientation of RotD100 is sampled from a uniform distribution, and hence all horizontal orientations are equally likely to be the orientation of RotD100. Other options for this sampling distribution could favor the strike-normal orientation (Shahi and Baker, 2014) or the transverse orientation (Poulos and Miranda, 2023). The orientation of RotD100 is assumed to be the same at all periods and for all buildings. Next, the angular distances ϕ_1 and ϕ_2 between the orientation of RotD100 and the two principal horizontal orientations of the building P_1 and P_2, respectively, are computed as shown in Figure 3a. Finally, at each period of the spectrum, the corresponding spectral ordinate at each principal horizontal orientation is computed as:

$$Sa_i = \nu(\phi_i)\, Sa_{\mathrm{RotD50}}, \quad i \in \{1,2\} \tag{1}$$

where Sa_{RotD50} is the corresponding RotD50 spectral acceleration; Sa_i is the spectral ordinate in the i-th principal orientation of the building; and $\nu(\phi_i)$ is a modification factor sampled from the four-parameter beta distributions calibrated by Poulos and Miranda (2022) using NGA-West2 ground motion records, which depend on angular distances ϕ_i and the period of vibration.

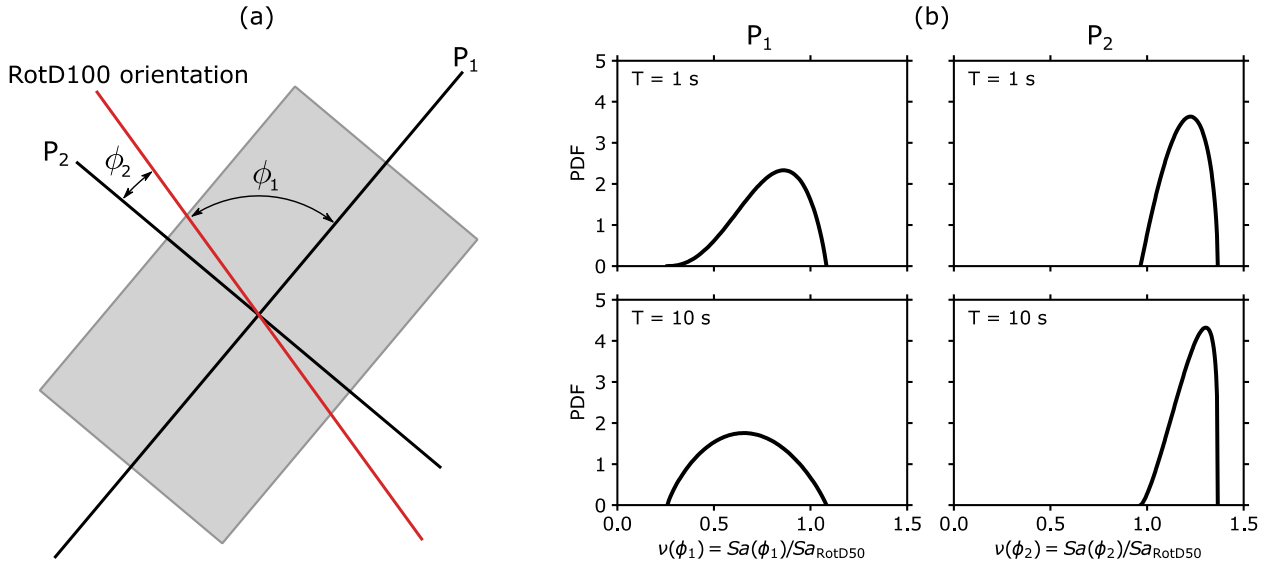

Figure 3. Sampling of response spectra in the two principal horizontal orientations of a building. (a) Schematical representation of a building floor plan with its two principal orientations (P_1 and P_2), the orientations of RotD100, and the corresponding angles between these orientations (ϕ_1 and ϕ_2). (b) Example sampling distributions for the ν ratios at periods of 1 and 10 s in the P_1 and P_2 orientations, obtained from Poulos and Miranda (2022).

2.2. Structural response

Each principal orientation of a building is modeled using the continuous non-uniform beam model developed by Taghavi and Miranda (2006) and improved by Alonso-Rodríguez and Miranda (2016), which consists of a shear beam coupled with a flexural beam. The model is fully defined by only four parameters: (1) the ratio between the shear and the flexural rigidities at the base of the building, α; (2) the ratio between the lateral stiffness at the top and the base of the building, δ; (3) the fundamental period; and (4) the damping ratio of the fundamental mode of vibration. For this study, α is sampled from a uniform distribution between 0 and 5 and δ is assumed to have the following deterministic relationship with the height of the building:

$$\delta = \max\{0.01, 0.35 - 0.001h\} \tag{2}$$

where h is the height of the building in meters. The fundamental period of the building is sampled from a model calibrated using system identification data from building responses in California (Cruz, 2017). The fundamental periods in each principal orientation of the building, T_{P1} and T_{P2}, are sampled using the following equation:

$$\ln(T_{Pi}) = a_T + b_T \ln(h) + \sigma_T \varepsilon_i, \quad i \in \{1,2\} \tag{3}$$

where coefficients a_T = -3.4514, b_T = 0.9290, and σ_T = 0.2865 were fitted using empirical data, and ε_i is sampled for both principal orientations simultaneously using a bivariate normal distribution to consider the correlation between the fundamental period in both orientations:

$$\begin{bmatrix}\varepsilon_1 \\ \varepsilon_2\end{bmatrix} \sim \mathcal{N}_2\left(\begin{bmatrix}0 \\ 0\end{bmatrix}, \begin{bmatrix}1 & \rho_T \\ \rho_T & 1\end{bmatrix}\right), \quad i \in \{1,2\} \tag{4}$$

where ρ_T = 0.8926 was fitted using the empirical data. The damping ratios of the fundamental modes in the two principal horizontal orientations of the building are sampled in the same way as the fundamental periods but with different coefficients:

$$a_\xi = -1.8606, \qquad b_\xi = -0.4393, \qquad \sigma_\xi = 0.2855, \qquad \rho_\xi = 0.4058 \tag{5}$$

Damping ratios of higher modes are sampled using the model developed by Cruz and Miranda (2017) for steel-braced frame buildings:

$$\xi_j = \xi_1 \left[1 + 0.13 \left(\frac{T_1}{T_j} - 1 \right) + 0.44\varepsilon \right], \quad j > 1 \tag{6}$$

where ξ_j is the damping ratio at the j-th mode, T_j is the period of the j-th mode, and ε is a sample from a standard normal random variable. Equation (6) accounts for the fact that damping ratios of higher modes tend to be higher than those of the first mode and that they tend to increase linearly with increasing frequency.

Once the period and damping ratio of each mode are sampled, spectral accelerations at each mode are obtained by first interpolation the response spectrum at the modal period and then using a damping modification factor from the model developed by Rezaeian et al. (2014):

$$Sa(T_j, \xi_j) = Sa_{5\%}(T_j) C(T_j, \xi_j) \tag{7}$$

where $Sa(T_j, \xi_j)$ is the spectral acceleration corresponding to the j-th mode, $Sa_{5\%}(T_j)$ is the 5%-damped spectral acceleration at the period of the j-th mode, and $C(T_j, \xi_j)$ is the damping modification factor sampled using a lognormal probability distribution with parameters given by Rezaeian et al. (2014). This study considered 6 modes of vibration in each of the two principal orientations of a building.

Once all the previous variables are sampled, the response of the building in each principal horizontal orientation is computed using modal response spectrum analysis. The structural response outputs are the peak floor accelerations (PFAs) and interstory drift ratios (IDRs) along the height of the building. The modal combination rule used for IDRs is the square root of sum of squares (SRSS), whereas the rule used for PFAs is the improved complete quadratic combination (CQC) procedure of Taghavi and Miranda (2006).

2.3. Damage and loss estimation

The generic inventory of structural and nonstructural components developed by Ramirez and Miranda (2009) for high-rise buildings is used to populate the buildings considered in the analysis. In their story-based procedure, structural and nonstructural components are either drift- or acceleration-sensitive and their fragility curves, which are also given by Ramirez and Miranda (2009), are used to sample their damage states. At each story of the buildings, the number of each type of component is split equally in both principal orientations of the building. Since Ramirez and Miranda (2009) provide the repair cost of each component relative to the replacement cost of the story and not the number of components, the damage states of all components in a given story and principal orientation are assumed to be the same. Thus, after the damage states are sampled for each component type, the resulting repair cost is normalized by the replacement cost of the story. These repair costs are then added for all stories and both orientations to obtain the number of lost stories of the building. Finally, the lost stories of all buildings are added up to obtain the total number of lost stories for the complete building set, which is the output of the analysis and provides a quantitative measure of seismic loss for the set of buildings.

2.4. Sensitivity analysis

Previous sections mention several random variables that should be sampled for each simulation. These variables are summarized in Table 1, which also presents the probability distribution used for sampling and the number of random variables that need to be sampled for the complete building set. The numbers shown in Table 1 depend on the number of buildings (n_b = 196), periods (n_p = 22), modes of vibration (n_m = 6), number of stories (n_s = 30), and building components (n_c = 23).

Table 1. List of random variables sampled for each simulation.

Variable	Probability distribution	Number
RotD100 orientation	Uniform	1
ν ratios	Four-parameter beta	$2n_b n_p$
Fundamental periods	Bivariate normal	$2n_b$
Fundamental damping ratios	Bivariate normal	$2n_b$
Damping ratios at higher modes	Normal	$2(n_m - 1)n_b$
α ratios	Uniform	$2n_b$
Damping modification factor: C	Lognormal	$2n_b n_m$
Damage states	Categorical	$2n_b n_s n_c$

A variance-based sensitivity analysis was performed to evaluate the relative importance of each random variable (or group of random variables). The sensitivity to a random variable was measured using the total-effect Sobol index (Homma and Saltelli, 1996), which represents the proportion of the variance of the output variable (i.e., number of lost stories for the complete building set) contributed by a given random variable, including all interaction of any order with the rest of the random variables. The Sobol indices were estimated using a Monte Carlo-based estimation (Saltelli et al., 2010), where 500 simulations were used for each random variable. This analysis enables a comparison of the impact of variables related to directionality (e.g., orientation of RotD100 and ν ratios) to other sources of uncertainty usually considered in regional seismic risk analysis.

3. Results

The first analysis that was performed was to run 1000 simulations for each of the two building layouts, that is, for the case where building orientations are sampled from a uniform distribution and where all buildings are oriented north-south/east-west. Figure 4 shows the resulting number of lost stories (the output variable) as a function of the azimuth of RotD100, which was sampled using a uniform distribution. For the case where building orientations are sampled from a uniform distribution, shown in Figure 4a, the probability distribution of the number of lost stories seems to not depend on the sampled azimuth of RotD100. Indeed, a general trend between these two variables, computed using locally weighted scatterplot smoothing (LOWESS, Cleveland 1979), shows almost no variation of the output variable with changes in the orientation of RotD100. On the other hand, for the case where all buildings are oriented north-south/east-west shown in Figure 4b, the output variable is strongly dependent on the azimuth of RotD100. As expected, for this case, the LOWESS trend has maximum values in the north, east, south, and west directions. This is because, for these cases, the orientation of RotD100 coincides with one of the principal orientations of all buildings, and hence one of those principal orientations is subjected to the maximum ground motion intensity from all possible horizontal orientations. The minimum values occur when the azimuth of RotD100 is at 45° from the principal orientations of the buildings, which leads to both principal orientations of the buildings being subjected to approximately equal intensities that are lower than the RotD100 intensity, leading to smaller levels of building response and consequently also lower levels of damage. The panels on the right of Figure 4 present kernel density estimates of the probability density function of the number of lost stories and the associated standard deviation of the distribution. The standard deviation of the losses for the set of buildings whose orientation is random and sampled from a uniform distribution is approximately half of the standard deviation computed for the set of buildings which all have the same orientation and whose principal orientations coincide with the north-south and east-west orientations.

Figure 4 shows the effect of one of the variables (orientation of RotD100) on the output variable visually. This effect was compared with that of the rest of the random variables considered in the analysis by using a variance-based sensitivity analysis. Figure 5 presents this comparison for the case of buildings oriented north-south/east-west. Figure 5a shows how the total-effect Sobol index of each random variable varies with the number of buildings considered in the analysis. For each possible number of buildings shown in the figure (i.e., 1 to 196), 100 building subsets were randomly selected (without replacement), and the indices presented correspond to mean indices from all subsets. When only a few buildings are considered in the analysis, most of the output variance is explained by the uncertainty in the fundamental period of the buildings, and the rest of the random variables have a significantly lower contribution. As more buildings are considered in the analysis, the azimuth of RotD100 starts to contribute more to the output variance and the rest of the random variables become less important. For the case when all buildings are considered, shown in Figure 5b, the azimuth of RotD100 has by far the highest Sobol index, followed by the fundamental period, and the rest of the variables have much lower indices. Since the Sobol indices were computed with a finite number of simulations (i.e., 500 for each random variable), the computed Sobol index estimates have sampling errors, which were quantified using 95% confidence intervals computed using bootstrapping (Efron and Tibshirani, 1994) and are depicted in the figure.

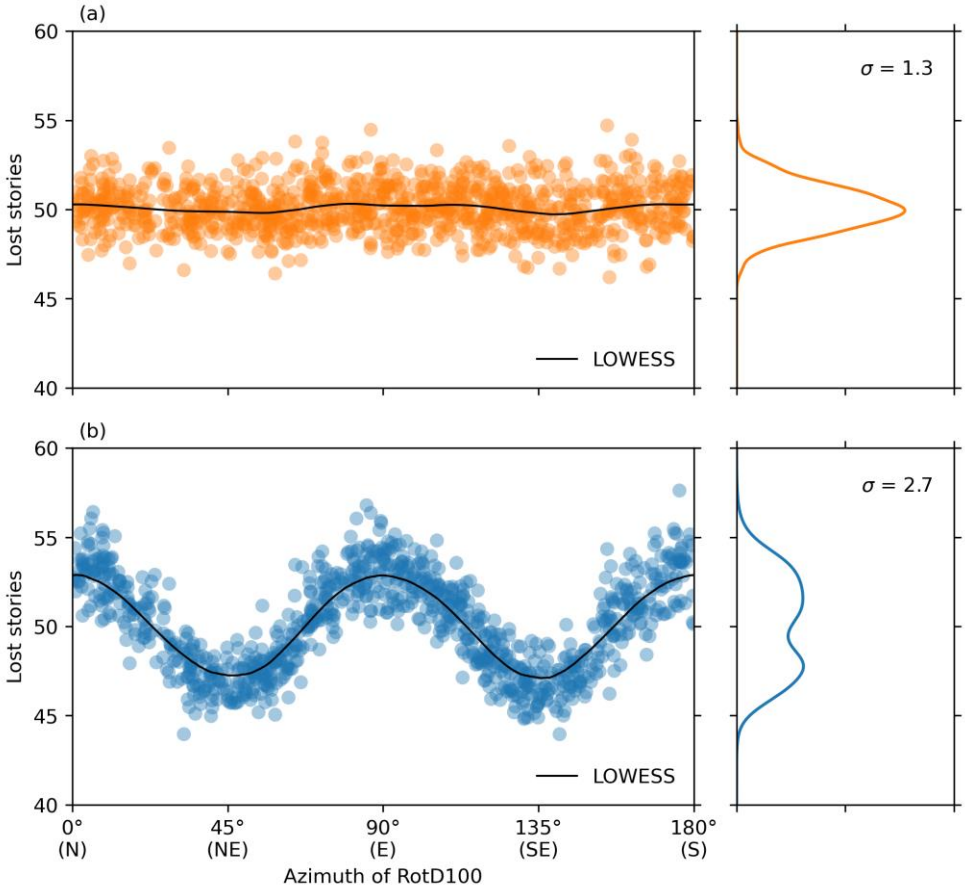

Figure 4. Variation of the number of lost stories with the azimuth of RotD100 for the case of buildings being: (a) having different orientations sampled from a uniform probability distribution; and (b) having the same orientations in a north-south/east-west grid. The right panels represent kernel density estimates of the distributions of lost stories.

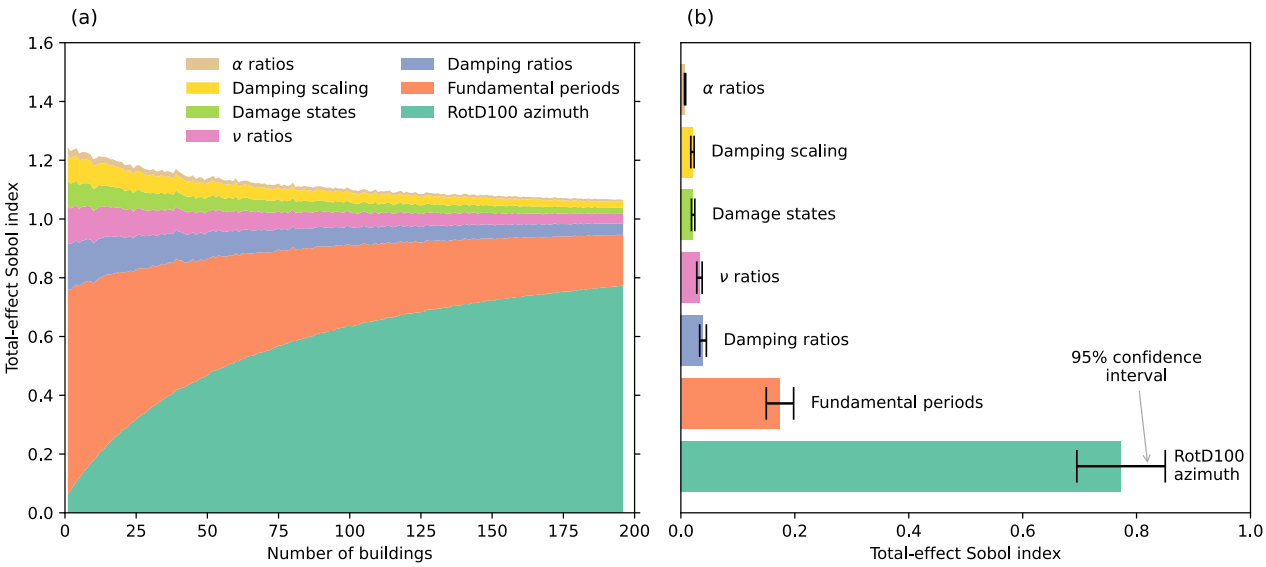

Figure 5. Total-effect Sobol indices of the seven considered random variables for the case of all buildings having the same orientations. (a) Variation of the indices with the number of buildings considered and (b) indices for all 196 buildings. Error bars represent 95% confidence intervals estimated using bootstrapping.

The fact that the azimuth of RotD100 starts to contribute more to the output variance, and therefore its Sobol index increases, as more buildings are considered in the analysis has to do with the number of times this random variable is being sampled. For a single simulation, the azimuth of RotD100 is sampled once and is used to compute the ϕ angles for all buildings, which are the same for the case in which all buildings have the same orientation. This introduces a correlation in building losses that increases the output variance. However, the rest of the random variables are sampled independently for each building, leading to a lower contribution to the output variance. Consequently, ground motion directionality, which is considered as a function of the angular distance between the orientation of RotD100 and the principal orientations of the buildings, becomes more important as more buildings are considered in the analysis.

4. Conclusions

This work studied the effect of ground motion directionality when estimating the seismic loss of a group of buildings within a city. A simulation-based probabilistic method was used to estimate the repair cost of a testbed consisting of a set of high-rise buildings. The method considers several sources of uncertainty, such as those related to ground motion directionality, structural response modeling, building damage, and loss assessment. For the testbed building set, the orientation of the maximum spectral response within the horizontal plane (i.e., the azimuth of Rot100), which was used to consider ground motion directionality within the analysis, was found to have a significant impact on seismic losses depending on building orientations. For the case where building orientations are randomly sampled using a uniform distribution, the azimuth of Rot100 had almost no effect on seismic losses. However, when all buildings had the same orientations, as it occurs in many cities or potions of large cities, the azimuth of Rot100 had a significant impact on seismic losses, with these losses being higher when the azimuth of RotD100 was close to one of the two principal orientations of the buildings. Since buildings in urban areas are usually orientated following street orientations, this implies that the layout of street networks within a city affects the variance of seismic losses, with rectangular grid layouts maximizing this variance.

The impact of the uncertainties related to ground motion directionality, and specifically the azimuth of RotD100, were compared to the impacts of the rest of the sources of uncertainty using a variance-based sensitivity analysis. The results show that, for the testbed building set with common orientations, the random variable that contributed the most to the variance of seismic losses is the azimuth of RotD100, and this contribution increased as more buildings were considered in the analysis.

The results of this study suggest that ground motion directionality should be considered in regional seismic risk analyses, especially when structures with relatively long periods (e.g., high-rise buildings) that are relatively close to each other (e.g., within the same city) are being analyzed. Almost all previous studies on regional seismic risk analysis have neglected ground motion directionality, and usually characterize ground motion intensity using central tendency measures (e.g., RotD50). However, the results of this study show that, under certain circumstances, uncertainties related to ground motion directionality can contribute significantly or even be the highest contributor to the variance of seismic losses, which is a compelling argument to consider ground motion directionality in these types of regional seismic risk analyses.

5. Acknowledgements

The authors thank Pablo Heresi for some initial discussions and for providing his code to perform regional seismic risk analysis, which was subsequently modified and expanded for this study. The doctoral studies of the first author were sponsored by the National Agency for Research and Development (ANID)/Doctorado Becas Chile/2019-72200307 and the Nancy Grant Chamberlain Fellowship at Stanford University.

6. References

Alonso-Rodríguez A., Miranda E. (2016). Dynamic behavior of buildings with non-uniform stiffness along their height assessed through coupled flexural and shear beams, *Bulletin of Earthquake Engineering*, 14(12), 3463-3483.

Baker J.W., Jayaram N. (2008). Correlation of spectral acceleration values from NGA ground motion models, *Earthquake Spectra*, 24(1), 299-317.

Boeing G. (2019). Urban spatial order: Street network orientation, configuration, and entropy, *Applied Network Science*, 4(1), 1-19.

Boore D.M. (2010). Orientation-independent, nongeometric-mean measures of seismic intensity from two horizontal components of motion, *Bulletin of the Seismological Society of America*, 100(4), 1830-1835.

Boore D.M., Stewart J.P., Seyhan E., Atkinson G.M. (2014). NGA-West2 equations for predicting PGA, PGV, and 5% damped PSA for shallow crustal earthquakes, *Earthquake Spectra*, 30(3), 1057-1085.

Cleveland W.S. (1979). Robust locally weighted regression and smoothing scatterplots, *Journal of the American statistical association*, 74(368), 829-836.

Cruz C. (2017). *Evaluation of damping ratios inferred from the seismic response of buildings*. PhD Thesis, Stanford University.

Cruz C., Miranda E. (2017). Evaluation of the Rayleigh damping model for buildings, *Engineering Structures*, 138, 324-336.

Efron B., Tibshirani R.J. (1994). *An introduction to the bootstrap*. New York: Chapman & Hall.

Heresi P., Miranda E. (2019). Uncertainty in intraevent spatial correlation of elastic pseudo-acceleration spectral ordinates, *Bulletin of Earthquake Engineering*, 17, 1099-1115.

Homma T., Saltelli A. (1996). Importance measures in global sensitivity analysis of nonlinear models, *Reliability Engineering & System Safety*, 52(1), 1-17.

Poulos A., Miranda E. (2022). Probabilistic characterization of the directionality of horizontal earthquake response spectra, *Earthquake Engineering & Structural Dynamics*, 51(9), 2077-2090.

Poulos A., Miranda E. (2023a). Effect of style of faulting on the orientation of maximum horizontal earthquake response spectra, *Bulletin of the Seismological Society of America*, 113(5), 2092-2105.

Poulos A., Miranda E. (2023b). Modification of ground-motion models to estimate orientation-dependent horizontal response spectra in strike-slip earthquakes, *Bulletin of the Seismological Society of America*. Advance online publication.

Poulos A., Miranda E., Baker J.W. (2022). Evaluation of earthquake response spectra directionality using stochastic simulations, *Bulletin of the Seismological Society of America*, 112(1), 307-315.

Ramirez C.M., Miranda, E. (2009). *Building-specific loss estimation methods & tools for simplified performance-based earthquake engineering*. Report No. 171, John A. Blume Earthquake Engineering Center, Stanford University.

Rezaeian S., Bozorgnia Y., Idriss I.M., Abrahamson N., Campbell K., Silva W. (2014). Damping scaling factors for elastic response spectra for shallow crustal earthquakes in active tectonic regions: “Average” horizontal component, *Earthquake Spectra*, 30(2), 939-963.

Saltelli A., Annoni P., Azzini I., Campolongo F., Ratto M., Tarantola S. (2010). Variance based sensitivity analysis of model output. Design and estimator for the total sensitivity index, *Computer Physics Communications*, 181(2), 259-270.

Shahi S.K., Baker J.W. (2014). NGA-West2 models for ground motion directionality, *Earthquake Spectra*, 30(3), 1285-1300.

Taghavi S., Miranda, E. (2006). *Probabilistic seismic assessment of floor acceleration demands in multi-story buildings*. Report No. 162, John A. Blume Earthquake Engineering Center, Stanford University.